Synthesis and Characterization of an Aza-cage Behaving as a 'Proton Sponge'. Crystal Structures of its Mono- and Tri-protonated Species

Andrea Bencini,[a] Antonio Bianchi,[a] Carla Bazzicalupi,[a] Mario Ciampolini,*[,a] Paolo Dapporto,[b] Vieri Fusi,[a] Mauro Micheloni,*[,c] Nicoletta Nardi,[a] Paola Paoli[b] and Barbara Valtancoli[a]

[a] *Department of Chemistry, University of Florence, Via Maragliano 75, I-50144, Italy*
[b] *Department of Energetics, University of Florence, Italy*
[c] *Institute of Chemical Sciences, University of Urbino, Italy*

The synthesis and characterization of the new macrobicyclic cage 4,10-dimethyl-1,4,7,10-tetraazabicyclo[5.5.4]hexadecane **L** is reported. Its basicity behaviour in aqueous solution has been investigated by potentiometric (25 °C, I = 0.15 mol dm^{-3}) and NMR (^{1}H and ^{13}C) techniques. It behaves as a very strong base (proton sponge) in the first protonation step, and as a moderate base in the second step (log K_2 = 7.8). ^{1}H–^{1}H and ^{1}H–^{13}C two-dimensional NMR experiments permitted the unequivocal assignment of all ^{1}H proton and ^{13}C resonances of both species HL^+ and H_2L^{2+}. Furthermore NMR experiments indicate that the first protonation involves the bridgehead nitrogens. Crystals of $[HL][ClO_4]$ are orthorhombic, space group $P2_1cn$, with a = 9.044(2), b = 12.573(2), c = 16.126(3) Å, and Z = 4; final R value of 0.089 (R_w = 0.086) for 1267 unique observed reflections with $I > 3\sigma(I)$. X-Ray analysis shows that protonation occurs on the bridgehead nitrogen N(2) and an overall macrocyclic conformation with the all nitrogen atoms in the *endo* configuration. The short H(2)···N(4) [1.69(1) Å] and N(2)···N(4) [2.75(1) Å] distances indicate a strong hydrogen bond. H(2) further interacts with the other two tertiary nitrogens: H(2)···N(1) [2.53(1) Å] and H(2)···N(3) [2.46(1) Å]. This arrangement makes the monoprotonated species very stable from the thermodynamic point of view and explains the high basicity of **L**. Crystals of $[H_3L][ClO_4]_3$ are tetragonal, space group $P4_32_12$, with a = 8.498(2), b = 8.498(2), c = 32.855(8) Å, and Z = 4; final R value of 0.083 (R_w = 0.093) for 1076 unique observed reflections with $I > 3\sigma(I)$. The X-ray analysis shows an overall macrocyclic conformation with two nitrogen atoms in the *endo* configuration and two in *exo* configuration.

Many small aza-cages have been extensively investigated by us in the last few years.[1–9] Proton-transfer and metal-complex formation properties of these compounds have been rationalized in terms of molecular topology, cavity size and nature of donor atoms. Most of these cages are selective, strong lithium binders, and a few of them have been found to behave as 'fast proton sponges'. To shed further light on the basicity behaviour we have synthesized the new cage 4,10-dimethyl-1,4,7,10-tetraazabicyclo[5.5.4]hexadecane, hereafter abbreviated as **L** (see Fig. 1).

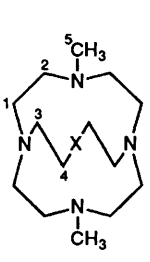

Apical group X	
None	(L)
—CH_2–NH–CH_2—	(L1)
—CH_2–O–CH_2—	(L2)
—$(CH_2)_3$—	(L3)
—CH_2–S–CH_2—	(L4)
—CH_2–N(CH_3)–CH_2—	(L5)
—NH—	(L6)
—N(CH_3)—	(L7)
—N(Bz)—	(L8)

Fig. 1 Structure of **L** with the atom labelling used in the ^{1}H and ^{13}C NMR studies

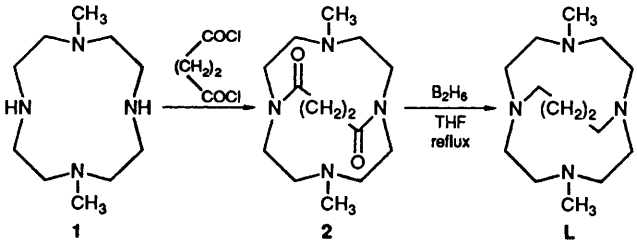

Fig. 2 Reaction sequence for the synthesis of the macrobicycle 4,10-dimethyl-1,4,7,10-tetraazabicyclo[5.5.4]hexadecane (**L**)

Experimental

Synthesis of **L**.—The reaction sequence to obtain **L** is reported in Fig. 2, and was an adaptation of similar procedures described in refs. 3 and 6 for related compounds. The starting macrocyclic compound 1,7-dimethyl-1,4,7,10-tetraazacyclododecane (**1**) was prepared as already described.[10]

Bicyclic Diamide **2**.—A sample (2.74 g, 0.0136 mol) of the *trans*-dimethylated tetraazamacrocycle **1** and triethylamine (8 cm^3) in dry benzene (500 cm^3) and succinyl chloride (2.12 g, 0.0136 mol) (Fluka) in dry benzene (500 cm^3) were added simultaneously to 1 dm^3 of dry benzene, with vigorous stirring, over a period of *ca.* 7 h at room temperature. The reaction mixture was filtered and then evaporated to dryness on a rotary evaporator. The crude product was extracted in hot cyclohexane and the resulting solution was concentrated; on cooling a white solid separated (2.45 g, 64%), m.p. 191–193 °C (Found: C, 59.5; H, 9.5; N, 19.8. Calc. for $C_{14}H_{26}N_4O_2$: C, 59.55; H, 9.28; N, 19.84%).

4,10-*Dimethyl*-1,4,7,10-*tetraazabicyclo*[5.5.4]*hexadecane Bis*(*hydroperchlorate*) $[H_2L][ClO_4]_2$.—A sample of BH_3·THF adduct [a solution of BH_3 0.1 mol in 100 cm^3 of tetrahydrofuran (THF)] was added dropwise, under a nitrogen atmosphere, to a solution of **2** (2.24 g, 7.9 mmol) in dry THF (30 cm^3) cooled to ice temperature. After removal of the cooling bath the reaction mixture was allowed to warm to room temperature and

Table 1 Crystal data and intensity collection parameters for [HL]·[ClO_4]

Formula	$C_{14}H_{31}ClN_4O_4$
M	354.9
Space group	$P2_1cn$
a/Å	9.044(2)
b/Å	12.573(2)
c/Å	16.126(3)
U/Å^3	1834(1)
Z	4
D_c/g cm^{-3}	1.29
F(000)	768
μ(Cu-Kα)/cm^{-1}	20.64
T	Ambient
Scan rate/deg min^{-1}	4
Scan mode	θ–2θ
Scan width/deg	0.7 + 0.15 tan θ
2θ range/deg	5–130
No. of reflections collected	1886
Unique obs. reflections [$I > 3\sigma(I)$]	1267
Refined parameters	211
R^a	0.089
$R_w{}^b$	0.086

^{a} $R = \Sigma||F_o| - |F_c||/\Sigma|F_o|$. ^{b} $R_w = [\Sigma w(|F_o| - |F_c|)^2/\Sigma wF_o^2]^{\frac{1}{2}}$.

Table 2 Crystal data and intensity collection parameters for [H_3L]·[ClO_4]$_3$

Formula	$C_{14}H_{33}Cl_3N_4O_{12}$
M	555.8
Space group	$P4_32_12$
a/Å	8.498(2)
b/Å	8.498(2)
c/Å	32.855(8)
U/Å^3	2373(1)
Z	4
D_c/g cm^{-3}	1.56
F(000)	1168
μ(Cu-$K\alpha$)/cm^{-1}	41.59
T	Ambient
Scan rate/deg min^{-1}	4
Scan mode	θ–2θ
Scan width/deg	1.1 + 0.15 tan θ
2θ range/deg	5–130
No. of reflections collected	1344
Unique obs. reflections [$I > 3\sigma(I)$]	1076
Refined parameters	159
R^a	0.083
$R_w{}^b$	0.093

^{a} $R = \Sigma||F_o| - |F_c||/|F_o|$. ^{b} $R_w = [\Sigma w(|F_o| - |F_c|)^2/\Sigma wF_o^2]^{\frac{1}{2}}$.

was then refluxed for 3 h. The solution was cooled and the excess of diborane was destroyed with a few drops of water. The solution was then evaporated to dryness, the white solid obtained was dissolved in HCl–H_2O–MeOH (6:9:30) and refluxed for 4 h. The resulting solution was evaporated to dryness and then the residue was dissolved in 5 cm^3 of water. The solution was made alkaline by addition of concentrated aqueous NaOH and extracted with chloroform (6 × 50 cm^3). The combined extracts were evaporated to dryness under reduced pressure to afford an oil. This was dissolved in ethanol (30 cm^3) and the dropwise addition of perchloric acid gave the diperchlorate salt, which was recrystallised from water–ethanol. Yield 2.49 g (69%) (Found: C, 37.4; H, 7.2; N, 12.5. Calc. for $C_{14}H_{32}Cl_2O_8$: C, 36.93; H, 7.08; N, 12.30).

Reagents.—NaCl (Merck *Suprapur*) was used as the ionic medium. Standardized CO_2-free solutions of NaOH were prepared according to the procedure already described.[11]

Potentiometric Measurements.—The potentiometric titrations were carried out with a fully automatic apparatus, as described in ref. 12. Two titration curves (152 data points) were used to determine the protonation constants of **L**. The computer program SUPERQUAD[13] was used to process the potentiometric data and calculate the protonation and stability constants.

NMR Spectroscopy.—A 200 MHz Bruker Ac-200 instrument was used to record the ^{13}C spectra at an operating frequency of 50.32 MHz.

Preparation of [HL][ClO_4].—The monoprotonated salt was obtained by extracting with chloroform an alkaline (NaOH) solution of [H_2L][ClO_4]$_2$. On slow evaporation of extracted solution, pure solid [HL][ClO_4] was obtained. Crystals of [HL][ClO_4] suitable for X-ray analysis were obtained by slow evaporation at room temperature of a solution containing [HL][ClO_4] in ethanol and a few drops of butanol.

Preparation of [H_3L][ClO_4]$_3$.—Crystals of [H_3L][ClO_4]$_3$ suitable for X-ray analysis were obtained from a 1 mol dm^{-3} $HClO_4$ solution which was allowed to stand at room temperature.

X-Ray Structure Analysis.—Analyses on single crystals of [HL][ClO_4] and [H_3L][ClO_4]$_3$ were carried out with an Enraf-Nonius CAD4 X-ray diffractometer; a summary of the crystallographic data is reported in Tables 1 and 2, respectively. Colourless crystals of approximate dimensions 0.3 × 0.2 × 0.1 mm and 0.4 × 0.4 × 0.2 mm of [HL][ClO_4] and [H_3L]-[ClO_4]$_3$, respectively, were mounted on the diffractometer and used for data collection at room temperature with graphite-monochromatized Cu-Kα radiation. Cell parameters of both compounds were determined by least-squares refinement of diffractometer setting angles for 25 carefully centred reflections. The intensities of three standard reflections were monitored periodically during data collection. Intensity data were corrected for Lorentz and polarization effects, an absorption correction was applied once the structures had been solved by using the Walker and Stuart method.[14] The structures were solved by direct methods using SIR88[15] and subsequently refined by the full-matrix least-squares technique. In both cases the function minimized was $\Sigma w(|F_o| - |F_c|)^2$, with $w = a/\sigma^2(F)$ and $w = a/[\sigma^2(F) + 0.001F^2]$, where a is an adjustable parameter, for [HL][ClO_4] and [H_3L][ClO_4]$_3$, respectively.

[HL][ClO_4]. The crystals of the compound belong to the orthorhombic family, space group $P2_1cn$. A ΔF map calculated in the final stage of the refinement showed unambiguously the presence of an hydrogen atom bound to an N-bridgehead atom. The other hydrogen atoms were introduced in calculated positions and their coordinates refined in agreement with those of the linked atoms, with a temperature factor U of 0.08 Å^2. Anisotropic thermal parameters were used with all the other non-hydrogen atoms. The final agreement factors were $R = 0.089$ and $R_w = 0.086$. Table 3 shows the final coordinates with estimated standard deviations.

[H_3L][ClO_4]$_3$. The compound crystallizes in the tetragonal crystal family; the ambiguity about the space group choice ($P4_32_12$ or $P4_12_12$) was solved during structure refinement. The $[H_3L]^{3+}$ cation is localized around a crystallographic twofold axis perpendicular to the C7–C7′ bond. A trace of disorder was found around the chlorine atom of a perchlorate anion lying on the twofold axis, therefore three oxygen atoms were included in the calculation to fit better the electron density map. Anisotropic temperature factors were used for all the atoms, except the hydrogen ones. The hydrogen atoms were

Table 3 Atomic coordinates (× 10^4) of [HL][ClO_4], with estimated standard deviations in parentheses

Atom	x/a	y/b	z/c
Cl	9196(0)	2862(2)	6366(2)
O(1)	9300(29)	1876(9)	6408(13)
O(2)	9200(23)	3382(16)	7166(7)
O(3)	8068(17)	3371(14)	6054(8)
O(4)	446(25)	3345(10)	6025(12)
N(1)	873(10)	6627(6)	5979(5)
C(1)	1206(16)	7735(9)	5870(8)
C(2)	1108(15)	8287(9)	6634(8)
N(2)	9589(10)	8335(6)	6998(5)
C(3)	8931(14)	9406(9)	6907(8)
C(4)	7417(15)	9445(9)	6671(7)
N(3)	7151(13)	8901(7)	5897(5)
C(5)	5967(17)	8088(11)	5975(9)
C(6)	6323(15)	7160(11)	6321(11)
N(4)	7853(10)	6755(7)	6334(5)
C(7)	8226(17)	6523(11)	5501(9)
C(8)	9851(17)	6188(11)	5389(8)
C(9)	2162(15)	5953(9)	6071(7)
C(10)	6939(19)	9640(10)	5219(7)
C(11)	9609(19)	8038(10)	7875(7)
C(12)	9574(23)	6912(10)	8042(7)
C(13)	8351(19)	6180(11)	7800(8)
C(14)	8025(19)	5915(9)	6957(10)

Table 4 Atomic coordinates (× 10^4) of [H_3L][ClO_4]$_3$ with estimated standard deviations in parentheses

Atom	x/a	y/b	z/c
Cl(1)	415(2)	5195(2)	−1172(1)
O(1)	352(12)	6063(11)	−1515(2)
O(2)	−728(9)	5760(9)	882(2)
O(3)	1918(12)	5421(17)	−990(3)
O(4)	−1(18)	3706(9)	−1276(3)
Cl(2)	6076(2)	6076(2)	0(0)
O(5)	6225(12)	4524(12)	−188(3)
O(61)[a]	5866(46)	6734(31)	−389(6)
O(62)[a]	6624(28)	7544(32)	−28(15)
N(1)	1667(6)	9492(7)	35(1)
C(1)	1466(10)	8325(9)	−302(2)
C(2)	1162(9)	9092(10)	−704(2)
N(2)	9472(8)	9100(7)	−839(2)
C(3)	8333(8)	9868(9)	−558(2)
C(4)	8709(9)	1562(9)	−442(2)
C(5)	9359(11)	9762(11)	−1266(2)
C(6)	3193(9)	386(12)	−1(2)
C(7)	3089(11)	2004(14)	133(2)

[a] Atom with population parameter of 0.5.

introduced in calculated positions, with an overall temperature factor of 0.05 Å^2, and their positional parameters varied according to those of the linked carbon atoms. The ΔF map carried out in the last refinement cycle did not allow us to localize the three hydrogen atoms of the [H_3L]$^{3+}$ cation. The convergence factors were R = 0.083 and R_w = 0.093. The final atomic coordinates are reported in Table 4.

All calculations, carried out on an IBM PS/2 computer model 80, were performed with the SHELX-76[16] set of programs which use the analytical approximation for the atomic scattering factors and anomalous dispersion corrections for all the atoms from the *International Tables for Crystallography*.[17] The molecular plots were produced by means of the ORTEP[18] program.

Tables of thermal parameters, hydrogen atom co-ordinates, observed and calculated structure factors (15 pages) have been deposited at the Cambridge Crystallographic Data Centre.*

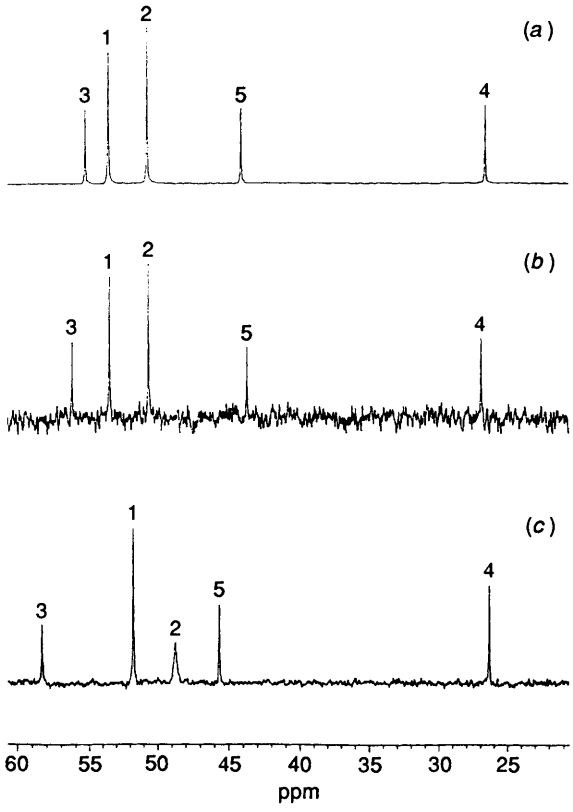

Fig. 3 ^{13}C NMR spectrum of [HL][Cl] (*a*) in $CDCl_3$; (*b*) in D_2O; (*c*) ^{13}C NMR spectrum of [H_2L][Cl]$_2$ in D_2O

Results and Discussion

Although the cage **L** is part of a series of well studied molecules,[1–9] its basicity behaviour is rather surprising. In aqueous solution it behaves as a diprotic base, the first protonation constant being unmeasurable because it is too high. In the second protonation step **L** behaves as a moderate base with log K_2 = 7.8(1) (see Table 5). Further protonation steps are insignificant under the experimental conditions employed in the potentiometric measurements (log K_3 < 2), although a triprotonated salt has been isolated in the solid state (see the Experimental section) and its crystal structure carried out. So far, only two other cages of the series (see Table 5) have been found to behave similarly to **L**, and have been termed 'fast proton sponges'.[1,2,4] The main goal of this investigation was to understand why **L** is a 'proton sponge', that is, to know how and where the proton is bound in the monoprotonated species [HL]$^+$. To achieve this we have carried out NMR studies at different pH and an X-ray analysis on the [HL][ClO_4] salt.

NMR Studies.—The ^{13}C NMR spectrum of **L**·HCl in $CDCl_3$ exhibits five sharp signals at 55.2 ppm (C3), 53.5 and 50.7 ppm (C1 and C2) 44.1 ppm (C5) and 26.6 ppm (C4), indicating a C_{2v} time-averaged symmetry [see Fig. 3(*a*)]. The ^{1}H NMR spectrum shows a complex multiplet at 3.03–2.86 ppm (eight protons), a multiplet at 2.83–2.78 ppm (four protons, assigned to the hydrogens of C3), a triplet at 2.63–2.57 ppm (eight protons), a singlet at 2.35 ppm (six protons, assigned to the hydrogen atoms of the methyl groups), a multiplet at 1.84–1.79 ppm (four protons, assigned to the hydrogens of C4), and finally a broad band at 13.0 ppm (integrating one proton), due

* For details of the CCDC deposition scheme see 'Instructions for Authors (1992),' *J. Chem. Soc., Perkin Trans. 2*, 1992, issue 1.

Table 5 Basicity constants (logarithms) of cages in aqueous solution, at 25 °C, I = 0.15 mol dm^{-3}

Reaction	Cage (see Fig. 1)								
	L	L1	L2	L3	L4	L5	L6	L7	L8
$H^+ + L = [HL]^+$	>14[a]	>14[b]	>14[c]	12.00[d]	11.91[e]	11.83[f]	12.48[g]	11.8[h]	11.8[i]
$[HL]^+ + H^+ = [H_2L]^{2+}$	7.8(1)	8.41	11.21	7.86	8.78	9.53	9.05	10.0	8.3

[a] This work, deprotonation of $[HL]^+$ in 1 mol dm^{-3} aqueous NaOH is undetectable. [b] Ref. 1. [c] Ref. 4. [d] Ref. 6. [e] Ref. 3. [f] Ref. 7. [g] Ref. 19. [h] Ref. 8. [i] Ref. 9.

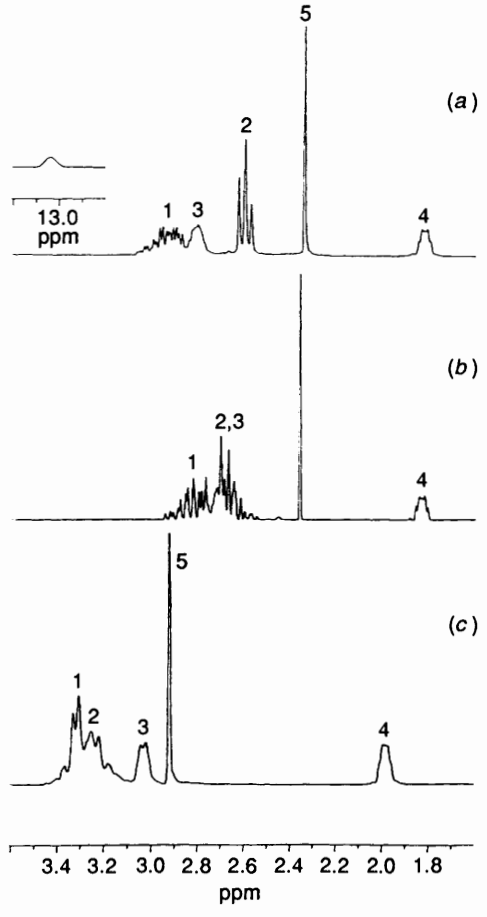

Fig. 4 ^{1}H NMR spectrum of [HL][Cl] (*a*) in $CDCl_3$; (*b*) in D_2O; (*c*) ^{1}H NMR spectrum of $[H_2L][Cl]_2$ in D_2O

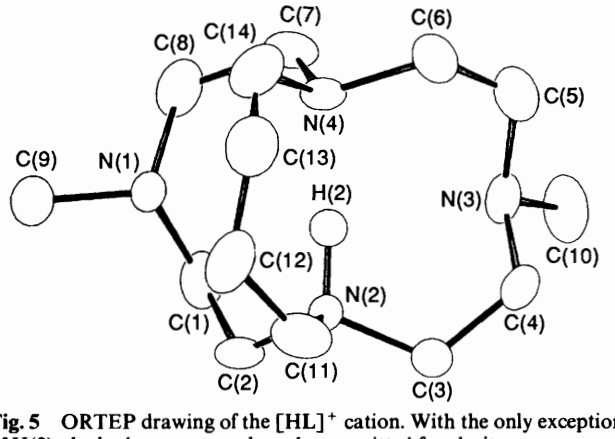

Fig. 5 ORTEP drawing of the $[HL]^+$ cation. With the only exception of H(2), the hydrogen atoms have been omitted for clarity

to the ammonium proton [see Fig. 4(*a*)]. By using the 2D ^{1}H–^{1}H homonuclear and ^{1}H–^{13}C heteronuclear correlations and homonuclear decoupling experiments, the ^{1}H and ^{13}C signals have been fully assigned, and the spectra are reported in Figs. 4(*a*) and 3(*a*), respectively.

A tentative hypothesis on the nitrogen atoms involved in the first protonation can be made. In a homonuclear decoupling experiment, the resonance at 1.81 ppm due to the hydrogens of C4 was selectively irradiated. In this situation the multiplet at 2.8 ppm, due to the hydrogens of C3, becomes a doublet. Addition of D_2O or MeOD to the chloroform solution of **L**·HCl, caused the resonance at 13.0 ppm to disappear and, on further decoupling of the signal of the hydrogens of C3 from the hydrogens of C4, the doublet at 2.8 ppm gives rise to a singlet, clearly indicating spin coupling between the NH proton and the hydrogen atoms of C3. As far as the ethylenic chain C1–C2 is concerned, decoupling of the signal of the hydrogens of C2 from those of C1, causes the triplet at 2.63–2.57 to become a singlet. No coupling between the NH^+ proton and the hydrogens of C2 was observed, the signal of methyl group being a sharp singlet. These spectral features indicate that for the monoprotonated species $[HL]^+$ the ammonium proton is localized on the bridgehead nitrogen atoms. The coupling constant between the NH hydrogen and the C3 hydrogens is estimated to be 2.8 Hz. Because of the C_{2v} time-averaged symmetry of the molecule, it can be concluded that the 'ammonium' proton is rapidly exchanged between the bridgehead nitrogens on the NMR timescale. We note that the NH^+ proton resonance (13.8 ppm) is at much lower field than those values of 9.3 ppm (**L1**)[1] and 10.1 ppm (**L8**)[4] found for NH^+ hydrogens in this kind of cage. A strong hydrogen bond, involving mainly the bridgehead nitrogens could explain this downfield shift. On addition of H_2O or MeOH to the chloroform solution of **L**·HCl, the NH resonance does not disappear, indicating that its exchange with mobile protons of these solvents is slow on the NMR timescale. This fact is rather unusual with the cages we have studied indicating an increased inertness toward deprotonation, probably as a result of increased strain of this cage and hydrophobic shielding of the ammonium group, due to the C_4 hydrocarbon chain. The proton exchange, however, is still quite rapid on the potentiometric measurements timescale.

The ^{13}C NMR spectrum of **L**·HCl in D_2O shows the same features as that in $CDCl_3$ [see Fig. 3(*b*)]. However the ^{1}H NMR spectrum displays a poorer resolution for the resonance of the hydrogens of C1, C2 and C3 [see Fig. 4(*b*)] and the disappearance of the signal due to the NH proton.

The ^{13}C NMR spectrum of **L**·2HCl in D_2O shows five signals at 58.3, 51.8, 48.7, 45.6 and 26.3 ppm. The ^{1}H NMR spectrum exhibits a complex multiplet at 3.4–3.1 ppm (16 protons, C1 and C2) a broad band at 3.05–2.95 ppm (four protons, C3), a singlet at 2.92 ppm (six protons, hydrogens of the methyl group) and a broad band at 2 ppm (four protons, hydrogens of C4). Using two-dimensional correlation it was possible to assign the signals of both the spectra [see Fig. 3(*c*) and 4(*c*)].

Crystal Structure of $[HL][ClO_4]$.—The crystal structure of the salt consists of discrete $[HL]^+$ cations and $[ClO_4]^-$ anions. Fig. 5 shows an ORTEP drawing of the $[HL]^+$ cation with the atom labelling. Bond lengths and angles are reported in Table 6. The most relevant information provided by the X-ray analysis is that relative to the protonation site, which is the bridgehead

Table 6 Selected bond distances /Å and angles/deg of $[HL][ClO_4]$, with estimated standard deviations in parentheses

N(1)–C(1)	1.44(1)	N(1)–C(8)	1.44(2)
N(1)–C(9)	1.45(2)	C(1)–C(2)	1.42(2)
C(2)–N(2)	1.50(2)	N(2)–C(3)	1.48(1)
N(2)–C(11)	1.46(1)	C(3)–C(4)	1.42(2)
C(4)–N(3)	1.44(1)	N(3)–C(5)	1.49(2)
N(3)–C(10)	1.45(1)	C(5)–C(6)	1.33(2)
C(6)–N(4)	1.47(2)	N(4)–C(7)	1.42(2)
N(4)–C(14)	1.47(2)	C(7)–C(8)	1.54(2)
C(11)–C(12)	1.44(2)	C(12)–C(13)	1.49(2)
C(13)–C(14)	1.43(2)		
C(8)–N(1)–C(9)	111(1)	C(1)–N(1)–C(9)	114(1)
C(1)–N(1)–C(8)	115(1)	N(1)–C(1)–C(2)	111(1)
C(1)–C(2)–N(2)	115(1)	C(2)–N(2)–C(11)	111(1)
C(2)–N(2)–C(3)	112(1)	C(3)–N(2)–C(11)	109(1)
N(2)–C(3)–C(4)	116(1)	C(3)–C(4)–N(3)	112(1)
C(4)–N(3)–C(10)	111(1)	C(4)–N(3)–C(5)	112(1)
C(5)–N(3)–C(10)	114(1)	N(3)–C(5)–C(6)	118(1)
C(5)–C(6)–N(4)	122(1)	C(6)–N(4)–C(14)	111(1)
C(6)–N(4)–C(7)	106(1)	C(7)–N(4)–C(14)	119(1)
N(4)–C(7)–C(8)	113(1)	N(1)–C(8)–C(7)	116(1)
N(2)–C(11)–C(12)	116(1)	C(11)–C(12)–C(13)	125(1)
C(12)–C(13)–C(14)	123(1)	N(4)–C(14)–C(13)	120(1)

Table 7 Selected bond distances/Å and angles/deg of $[H_3L][ClO_4]_3$, with estimated standard deviations in parentheses

N(1)–C(1)	1.497(9)	N(1)–C(6)	1.507(11)
N(1)′–C(4)	1.494(8)	C(1)–C(2)	1.498(9)
C(2)–N(2)	1.503(10)	N(2)–C(3)	1.488(9)
N(2)–C(5)	1.504(9)	C(3)–C(4)	1.523(10)
C(6)–C(7)	1.447(20)	C(7)–C(7)′	1.572(14)
C(1)–N(1)–C(6)	112.0(5)	C(4)–N(1)′–C(6)′	110.3(5)
C(1)′–N(1)′–C(4)	111.1(5)	N(1)–C(1)–C(2)	112.6(6)
C(1)–C(2)–N(2)	115.3(6)	C(2)–N(2)–C(5)	109.7(6)
C(2)–N(2)–C(3)	116.2(5)	C(3)–N(2)–C(5)	112.5(6)
N(2)–C(3)–C(4)	115.7(6)	N(1)′–C(4)–C(3)	112.0(9)
N(1)–C(6)–C(7)	113.8(7)	C(6)–C(7)–C(7)′	115.0(7)

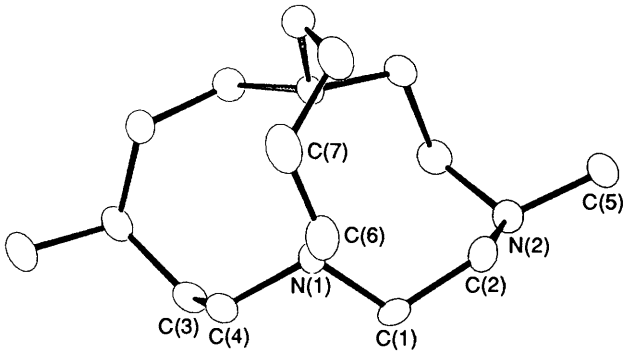

Fig. 6 ORTEP drawing of the $[H_3L]^{3+}$ cation. The hydrogen atoms have been omitted for clarity

nitrogen N(2), to which the hydrogen H(2) is bound. Notably these solid-state features are in full agreement with those found in NMR solution studies, where the two equivalent bridgehead nitrogens N(2) and N(4) were found to be involved in the first protonation step. The macrobicycle displays an overall conformation similar to that found for the monoprotonated species of **L1** and **L8**, with the nitrogen atoms in the *endo* configuration.[2,4] The short H(2)···N(4) distance [1.69(1) Å] indicates a rather strong hydrogen bond. The N(2)···N(4) distance is the shortest [2.75(1) Å] of the series and it is slightly longer than that found in the bicyclic diamine 1,6-diazabicyclo-[4.4.4]tetradecane (2.53 Å).[20] Furthermore H(2) interacts with the other two methylated nitrogens: H(2)···N(1) [2.53(1) Å] and H(2)···N(3) [2.46(1) Å]. The averaged hydrogen bond H(2)···N distance (2.23 Å) compares well with that found for the H···N distance (2.36 Å) of the monoprotonated penta-aza cage **L1**, which was found to behave as a 'fast proton sponge'.[1,2] For the other cage of the series, **L5**, which does not behave as a proton sponge, the mean hydrogen bond distances of the localized hydrogen in the monoprotonated species is 2.54 Å,[5] significantly longer than that found for **L**.

Crystal Structure of $[H_3L][ClO_4]_3$.—The crystal structure of the salt consists of discrete $[H_3L]^{3+}$ cations and independent $[ClO_4]^-$ anions. Fig. 6 shows an ORTEP drawing of the $[H_3L]^{3+}$ cation with the atom labelling. Selected bond lengths and angles are reported in Table 7. A comparison of the structure of the triply charged cation $[H_3L]^{3+}$ (see Fig. 6) with that of the singly charged $[HL]^+$ cation (see Fig. 5) allows us to explore the influence on the macrocyclic configuration of the addition of two extra charges. The distance between the bridgehead nitrogen atoms remains comparable, 2.75(1) Å and 2.624(8) Å for $[HL]^+$ and $[H_3L]^{3+}$, respectively, indicating the presence of a strong N–H···N hydrogen bond also in the latter species. In contrast the methylated nitrogen atoms in $[H_3L]^{3+}$ are separated more than in the $[HL]^+$ cation [5.531(7) *vs.* 4.42(1) Å] conferring an elliptical elongation to the macrocycle. This conformational feature confirms that while a hydrogen atom is shared by the two bridgehead nitrogens the other two hydrogen atoms are localized on the two methylated nitrogen atoms. As a consequence of this arrangement the two N(2) and N(2)′ atoms are in the *exo* configuration with the $N–H^+$ bonds pointing towards the outside of the cage cavity. The other possible disposition of the three charges, involving the protonation of both bridgehead nitrogen atoms and one of the two methylated nitrogens can be rejected because this requires a large distance between the bridgehead nitrogen atoms in sharp contrast with the experimental evidence.

Conclusions

The proton-transfer properties of **L** have been rationalized. The protonation sites have been located as one of the equivalent bridgehead nitrogens in the first protonation step and one of the methylated nitrogens in the second protonation step. The X-ray analysis of $[HL]^+$ indicates that the cage can adopt a conformation which allows the hydrogen atom H(2) bound to N(2) to form an hydrogen bond network, which makes the monoprotonated species very stable from the thermodynamic point of view and explains the high basicity in the first protonation step. The crystal structure of the triply protonated species $[H_3L]^{3+}$ indicates that the protonation sites involved are the two methylated nitrogen atoms and one of the bridgehead nitrogens.

Acknowledgements

We are indebted to MURST (*Ministero per l'Università e la Ricerca Scientifica e Tecnologica*) and CNR (*Consiglio Nazionale delle Ricerche*) for financial support.

References

1 S. Chimichi, M. Ciampolini, P. Dapporto, M. Micheloni, F. Vizza and F. Zanobini, *J. Chem. Soc., Dalton Trans.*, 1986, 505.
2 M. Ciampolini, S. Mangani, M. Micheloni, P. Orioli, F. Vizza and F. Zanobini, *Gazz. Chim. Ital.*, 1986, **116**, 189.
3 A. Bianchi, E. Garcia-España, M. Micheloni, N. Nardi and F. Vizza, *Inorg. Chem.*, 1986, **25**, 4379.

4 A. Bianchi, M. Ciampolini, M. Micheloni, N. Nardi, B. Valtancoli, S. Mangani, E. Garcia-España and J. A. Ramirez, *J. Chem. Soc., Perkin Trans. 2*, 1989, 1131.
5 A. Bencini, A. Bianchi, M. Ciampolini, E. Garcia-España, P. Dapporto, M. Micheloni, P. Paoli, J. A. Ramirez and B. Valtancoli, *J. Chem. Soc., Chem. Commun.*, 1989, 701; A. Bencini, A. Bianchi, A. Borselli, M. Ciampolini, E. Garcia-España, P. Dapporto, M. Micheloni, P. Paoli, J. A. Ramirez and B. Valtancoli, *Inorg. Chem.*, 1989, **28**, 4279.
6 A. Bencini, A. Bianchi, A. Borselli, M. Ciampolini, P. Dapporto, E. Garcia-España, M. Micheloni, P. Paoli, J. A. Ramirez and B. Valtancoli, *J. Chem. Soc., Perkin Trans. 2*, 1990, 209.
7 A. Bencini, A. Bianchi, A. Borselli, S. Chimichi, M. Ciampolini, P. Dapporto, M. Micheloni, N. Nardi, P. Paoli and B. Valtancoli, *J. Chem. Soc., Chem. Commun.*, 1990, 174.
8 A. Bencini, A. Bianchi, S. Chimichi, M. Ciampolini, P. Dapporto, M. Micheloni, N. Nardi, P. Paoli and B. Valtancoli, *Inorg. Chem.*, 1991, **30**, 3687.
9 A. Bencini, A. Bianchi, M. Ciampolini, P. Dapporto, M. Micheloni, N. Nardi, P. Paoli and B. Valtancoli, *J.Chem. Soc., Perkin Trans. 2*, 1992, 181.
10 M. Ciampolini, P. Dapporto, M. Micheloni, N. Nardi, P. Paoletti and F. Zanobini, *J. Chem. Soc., Dalton Trans.*, 1984, 1357.
11 M. Micheloni, A. Sabatini and A. Vacca, *Inorg. Chim. Acta*, 1977, **25**, 41.
12 M. Fontanelli and M. Micheloni, *Proceedings of the Spanish-Italian Congress on Thermodynamics of Metal Complexes*, Peñiscola, June 3–6 1990, *Departament de Quimica Inorganica*, University of Valencia, Spain, p. 41.
13 P. Gans, A. Sabatini and A. Vacca, *J. Chem. Soc., Dalton Trans.*, 1985, 1195.
14 N. Walker and D. D. Stuart, *Acta Crystallogr., Sect. A*, 1983, **39**, 158.
15 M. C. Burla, M. Camalli, G. Cascarano, C. Giacovazzo, G. Polidori, R. Spagna and D. Viterbo, *J. Appl. Cryst.*, 1989, **22**, 389.
16 G. M. Sheldrick, SHELX 76. *A Program for Crystal Structure Determination*, University of Cambridge, UK, 1976.
17 *International Tables for X-Ray Crystallography*, Kynoch Press, Birmingham, UK, 1974, vol. 4.
18 C. K. Johnson, ORTEP, Report ORNL 3794, Oak Ridge National Laboratory, Tennessee, USA, 1971.
19 A. Bencini, A. Bianchi, A. Borselli, S. Chimichi, M. Ciampolini, P. Dapporto, M. Micheloni, N. Nardi, P. Paoli and B. Valtancoli, *Inorg. Chem.*, 1990, **29**, 3282.
20 R. W. Alder, A. G. Orpen and R. B. Sessions, *J. Chem. Soc., Chem. Commun.*, 1983, 999.

Paper 2/03158B
Received 16*th June* 1992
Accepted 15*th September* 1992